Biological Psychiatry: CNNI

Archival Report

Longitudinal Analysis of Brain Function-Structure Dependencies in 22q11.2 Deletion Syndrome and Psychotic Symptoms

Silas Forrer, Farnaz Delavari, Corrado Sandini, Halima Rafi, Maria Giulia Preti, Dimitri Van De Ville, and Stephan Eliez

ABSTRACT

BACKGROUND: Compared with conventional unimodal analysis, understanding how brain function and structure relate to one another opens a new biologically relevant assessment of neural mechanisms. However, how function-structure dependencies (FSDs) evolve throughout typical and abnormal neurodevelopment remains elusive. The 22q11.2 deletion syndrome (22q11.2DS) offers an important opportunity to study the development of FSDs and their specific association with the pathophysiology of psychosis.

METHODS: Previously, we used graph signal processing to combine brain activity and structural connectivity measures in adults, quantifying FSD. Here, we combined FSD with longitudinal multivariate partial least squares correlation to evaluate FSD alterations across groups and among patients with and without mild to moderate positive psychotic symptoms. We assessed 391 longitudinally repeated resting-state functional and diffusion-weighted magnetic resonance images from 194 healthy control participants and 197 deletion carriers (ages 7–34 years, data collected over a span of 12 years).

RESULTS: Compared with control participants, patients with 22q11.2DS showed a persistent developmental offset from childhood, with regions of hyper- and hypocoupling across the brain. Additionally, a second deviating developmental pattern showed an exacerbation during adolescence, presenting hypocoupling in the frontal and cingulate cortices and hypercoupling in temporal regions for patients with 22q11.2DS. Interestingly, the observed aggravation during adolescence was strongly driven by the group with positive psychotic symptoms.

CONCLUSIONS: These results confirm a central role of altered FSD maturation in the emergence of psychotic symptoms in 22q11.2DS during adolescence. The FSD deviations precede the onset of psychotic episodes and thus offer a potential early indication for behavioral interventions in individuals at risk.

https://doi.org/10.1016/j.bpsc.2024.05.008

Cognitive processes are the result of dynamic interactions between brain regions that communicate with each other via structural pathways and neuronal activations (1,2). While brain function is expressed on and constrained by the structural white matter pathways (3), the degree to which the former is bound by the underlying structure remains a topic of ongoing research (4,5).

Recent studies showed that the coupling strength between structure and function follows a macroscale spatial gradient that spans from more strongly coupled in lower sensory regions to more strongly decoupled in high-level cognitive ones (6,7), which follows the concept of a sensorimotor-association axis (8). Variations in coupling strength across different regions of the brain's macroscale gradient are rooted in regional differences consistent with specific functions in those brain regions (9). In particular, the increased coupling strength of sensorimotor areas is consistent with rapid and reliable neuronal responses to both external and internal stimuli. In contrast, activity in regions involved in higher-order cognitive processes such as episodic memory or self-referential thoughts, which are more variable, exhibit greater decoupling from the underlying structure (6). Therefore, the coupling strength serves as an informative indicator regarding the putative function of the respective brain region. Insights gained from the coupling strength are not only crucial for understanding the normative functioning of the brain but also hold implications for investigating alterations due to neurological disease and disorders, e.g., the emergence of psychotic symptoms in schizophrenia (10). Abnormal integration between brain regions (i.e., dysconnectivity) on both a structural and functional level is a consistently proposed key mechanism in psychosis (11–15). Primary findings on the emergence of psychotic symptoms in schizophrenia have revealed a reduction in both anatomical and functional connectivity that is notably evident in frontotemporal connectivity (16–19).

However, considering functional and structural connectivity separately ignores potentially relevant information about their interaction (20,21). The investigation of the coupling strength

SEE COMMENTARY ON PAGE 849

between structure and function is a promising approach to provide further insights into the neurobiological mechanisms that underlie psychosis. In a smaller cross-sectional study (7), we investigated functional-structural coupling in adults with 22q11.2 deletion syndrome (22q11.2DS) and its contribution to positive psychotic symptoms (PPSs). 22q11.2DS is a neurogenetic disorder that is among the strongest genetic risk factors for developing psychosis (22). Approximately 30% to 40% of deletion carriers are diagnosed with schizophrenia by adulthood (23–25). Moreover, 22q11.2DS is usually diagnosed at a young age due to frequently associated heart or cleft palate malformations (26). Studies on this population constitute a unique opportunity to map the early stages and the progression of psychosis (27).

The results of our initial study in adults with 22q11.2DS showed an association between the presentation of PPSs and weaker coupling in the cingulate gyrus and the parietal lobule, while stronger coupling was observed in the temporal gyrus (7). This provided the first evidence regarding how altered expression of brain function on the underlying structure could be informative in identifying the neurobiological targets that contribute to psychosis. However, there are no insights into the developmental emergence of these alterations. Nevertheless, it is crucial to adopt a neurodevelopmental perspective when investigating psychosis. Recent studies suggest that prodromal symptoms of psychosis could emerge during early adolescence, considering psychotic symptoms as a late, potentially preventable stage of the illness (28–30). Therefore, here we employed a developmental longitudinal study to explore the neurodevelopmental trajectory of function-structure coupling in both healthy control individuals and individuals with 22q11.2DS across a wide age range, spanning from childhood to adulthood.

We employed the same methodology as outlined in Preti and Van de Ville (6), utilizing resting-state functional and diffusion magnetic resonance images (MRIs). This method integrates brain function and structure measures to explore the degree to which brain activity in specific regions relies on underlying white matter connections. We quantified regional function-structure dependency (FSD) and examined its developmental trajectories and deviations in patients with 22q11.2DS compared with healthy control participants (HCs) using multivariate partial least squares correlation (PLS-C) analysis. Given the absence of prior knowledge regarding developmental deviations, our objective was to identify patterns that underwent the most significant developmental changes. To achieve this, we constructed the PLS behavior side with regressors representing age and age × diagnosis interactions. The PLS method was chosen for its capability to uncover relationships between 2 data matrices (31). This approach is particularly well suited for our study, which involves longitudinal analysis in which we utilized age alongside measures of brain activity. This approach allowed us to discern whether changes in FSD were an early manifestation or a consequence of neurodevelopmental processes. We aimed to identify critical time windows in development during which significant FSD changes occurred between patients and control participants. Moreover, we investigated how FSD maturation patterns differed across deletion carriers with and without mild to moderate PPSs.

Building on previous research in psychosis and 22q11.2DS, which accentuate consistent involvement of the frontal-cingulate, parietal, and temporal cortices (32,33), and based on the findings of our initial study on FSD in adults with 22q11.2DS (7), we hypothesized that patients with 22q11.2DS would exhibit increased FSD in temporal regions and decreased FSD in frontal-cingulate regions and the parietal lobule. We expected these changes to emerge prominently during adolescence because it has been repeatedly documented that adolescence is a critical period for brain development and further the peak age of onset in psychiatric disorders (30,33). Furthermore, we expected to see higher FSD deviations in participants who later develop PPSs, which may serve as a biomarker to aid the development of interventions in the early stages of psychosis.

METHODS AND MATERIALS

Participants

The dataset comprised multimodal imaging and behavioral data from 233 participants, including 108 participants with a genetically confirmed diagnosis of 22q11.2DS (50 females, age range: 7.3–34.0 years) and 125 HCs (68 females, age range: 7.4–33.2 years). The number of longitudinal assessments varied between 1 and 5, resulting in 391 longitudinal assessments (197 for 22q11.2DS carriers and 194 for HCs, collected over a span of 12 years) overall. Participants' demographic and clinical characteristics are summarized in Table 1. A detailed overview of medication use within patients is summarized in Table 2. Written informed consent was obtained from participants and/or their parents. The study was approved by the cantonal ethics committee and was conducted according to the Declaration of Helsinki.

MRI Acquisition and Processing

Structural and functional MRI data, including T1, resting-state functional MRI (rs-fMRI), and diffusion MRI (dMRI) were acquired using a 3T Siemens Trio (n = 265) and a 3T Siemens Prisma-fit (MAGNETOM Trio Upgrade) (n = 126) scanner. See Supplemental Methods for details about used sequence parameters. rs-fMRI data were processed using SPM12 (http://www.fil.ion.ucl.ac.uk/spm/) and the Data Processing Assistant for rs-fMRI. Voxels were averaged using 200 cortical (34) and 32 subcortical (35) regions of interest (ROIs). A bandpass filter (0.01–0.1 Hz) was applied, resulting in resting-state functional time courses for each ROI. An explanation of the rs-fMRI processing pipeline is provided in Supplemental Methods.

dMRI and T1 images were processed with an in-house pipeline using a combination of Mrtrix3 (http://www.mrtrix.org/) (36) and FSL (37). Processing included the following steps: 1) extraction of the brain based on T1 images, 2) warping of the parcellated ROIs from Montreal Neurological Institute to T1 subject space, 3) transforming T1 and ROIs to dMRI subject space, 4) fiber tracking with the probabilistic tractography method, and 5) generation of the parcellated connectome (232 ROIs). An explanation of the diffusion-weighted MRI processing pipeline is provided in the Supplemental Methods.

Table 1. Participant Characteristics

Demographic Variable	22q11.2DS Group, *n* = 108	Healthy Control Group *n* = 125	*p* Value
Sex (Female/Male)	108 (50/58)	125 (68/57)	.22[a]
No. of Scans (Female/Male)	197 (97/100)	194 (90/104)	.39[a]
Participants With 1 Scan	52	70	NA
Participants With 2 Scans	31	41	NA
Participants With 3 Scans	18	14	NA
Participants With 4 Scans	6	0	NA
Participants With 5 Scans	1	0	NA
Average Time Between Longitudinal Visits, Years	4.10 (1.44)	4.01 (1.18)	.68[b]
PPS(+) Participants (Female/Male)	52 (23/29)	0	.71[a]
PPS(−) Participants (Female/Male)	48 (23/25)	0	
Scanner Type, Prisma-Fit/Trio	71/126	55/139	.10
Average Age, Years	18.65 (5.66)	17.70 (5.79)	.10
Average IQ	71.96 (12.56)	112.15 (13.51)	<.001[c]
Motion: Average FD After Scrubbing	0.17 (0.05)	0.13 (0.04)	<.001[c]
Anxiety Disorder[d]	56 (51.9%)	0	NA
Attention-Deficit/Hyperactivity Disorder[d]	57 (52.8%)	0	NA
Mood Disorder[d]	25 (23.2%)	0	NA
Schizophrenia Spectrum Disorders[d]	10 (9.3%)	0	NA
More Than 1 Psychiatric Comorbidity[d]	48 (44.4%)	0	NA
Anticonvulsants[d]	4 (3.7%)	0	NA
Antidepressants[d]	27 (25.0%)	0	NA
Neuroleptic[d]	17 (15.7%)	0	NA
Psychostimulant[d]	41 (38.0%)	0	NA
Anxiolytic[d]	5 (4.6%)	0	NA
Antiepileptic[d]	3 (2.8%)	0	NA

Values are presented as *n*, *n* (%), or mean (SD). IQ was measured using the Wechsler Intelligence Scale for Children-III (94) and Wechsler Adult Intelligence Scale-III (95) for adults. Presence of psychiatric disorders was assessed through clinical interview with patients using the Diagnostic Interview for Children and Adolescents–Revised (96), the psychosis supplement from the Schedule for Affective Disorders and Schizophrenia for School-Age Children–Present and Lifetime version (97), and the Structured Clinical Interview for DSM-IV Axis I disorders (98).

22q11.2DS, 22q11 deletion syndrome; FD, framewise displacement; NA, not available; PPS, positive psychotic symptom.

[a]Calculated first-level average within-participant measurements, and then second level across all participants.

[b]Significant at $p < .05$ (χ^2 test).

[c]Significant at $p < .05$ (*t* test).

[d]Positive if present at any of the assessments.

Function-Structure Dependency

As illustrated in Figure 1A–D, for each participant visit, we computed the structural decoupling index (SDI) for each ROI, which indicates the degree of functional signal alignment with underlying brain structure. Using graph signal processing methods [detailed in (6) and in the Supplement], we obtained structural patterns known as structural harmonics. These were used to project fMRI activity onto structural patterns, thereby expressing the functional signal as a weighted sum of the structural patterns. Next, we split functional activity into components coupled and decoupled from structure based on structural harmonic frequency. The $\log_2$ of their ratio (decoupled over coupled) yielded the FSD, with negative FSD for SDI < 1 and positive FSD for SDI > 1.

Table 2. Overview of Medication Intake Between PPS(+) and PPS(−) Patients

Demographic Variable	PPS(+)	PPS(−)	*p* Value
Anticonvulsants[a]	3 (5.77%)	1 (2.08%)	.347
Antidepressants[a]	19 (36.54%)	8 (16.67%)	.025[b]
Neuroleptic[a]	14 (26.92%)	3 (6.25%)	.006[b]
Psychostimulant[a]	23 (44.23%)	18 (37.50%)	.494
Anxiolytic[a]	4 (7.69%)	1 (2.08%)	.200
Antiepileptic[a]	2 (3.85%)	1 (2.08%)	.606
At Least 1 Type of Medication	34 (65.38%)	19 (39.58%)	.010[b]

Values are presented as *n* (%).

PPS, positive psychotic symptom.

[a]Positive if present at any of the assessments.

[b]Significant at $p < .05$ (χ^2 test).

Clinical Assessment

To investigate the significance of individual developmental trajectories of FSD for proneness to psychosis, we created PPS(+) and PPS(−) subgroups using the Structured Interview for Prodromal Syndromes, an adapted and validated instrument in 22q11.2DS (38,39). This clinical tool was used to assess the presence and the severity of PPSs at each time point. The positive subscale includes the following 5 symptoms: unusual thought content, suspiciousness, grandiose ideas, hallucinations, and disorganized communication. Eight

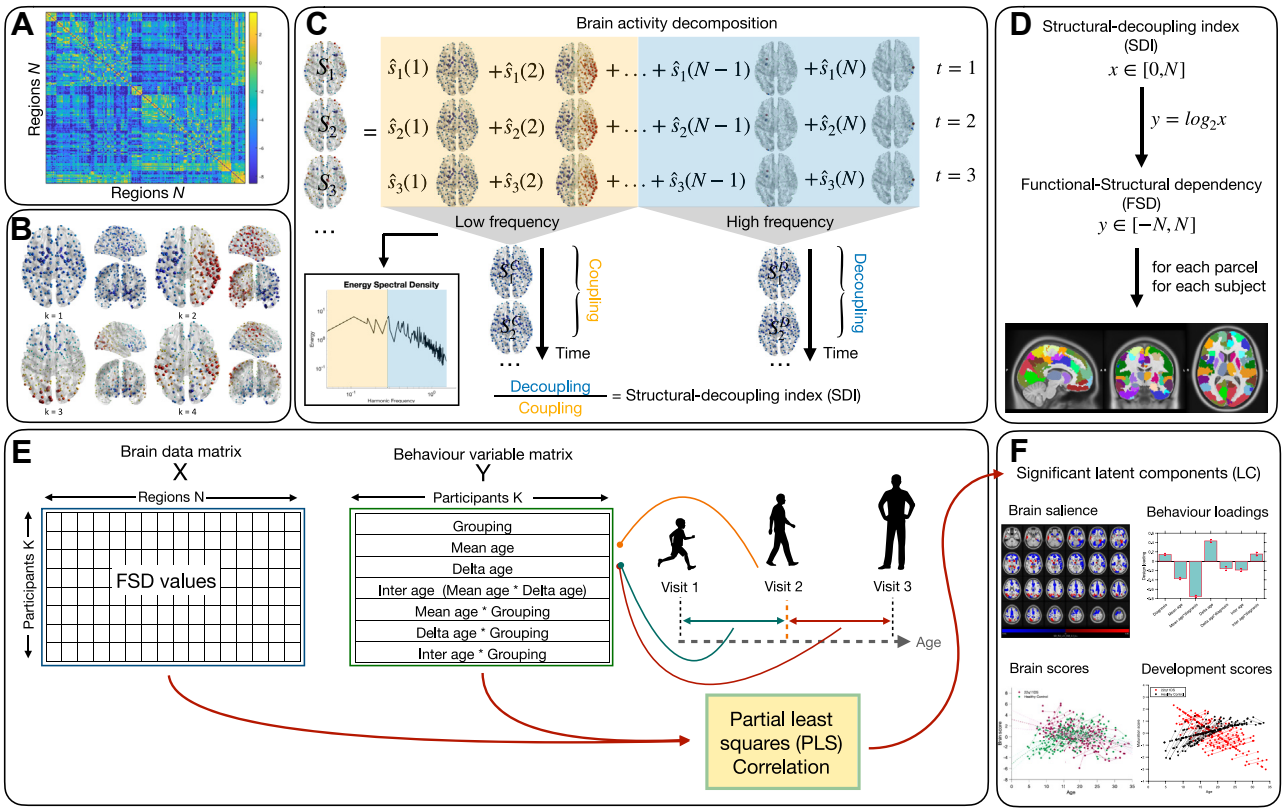

Figure 1. Method pipeline. **(A)** SC in 232 atlas regions. **(B)** SC eigendecomposition led to structural harmonics with increasing spatial frequency *k*. **(C)** Brain activity at every time point $t(s_t)$ was written as a linear combination of harmonics [by using coefficients $\hat{s}(t)$]. The median-split criterion on the activity energy spectral density ξ (inset) was used to split the spectrum and decompose brain activity into coupled/decoupled portions s_t^C and s_t^D (using low/high-frequency harmonics, respectively; λ = harmonic frequency). The ratio between decoupled/coupled signal norms is defined as the SDI. **(D)** A binary logarithm was applied on structural decoupling indices to obtain FSD values; negative FSD for SDI < 1 and positive FSD for SDI > 1. **(E)** Design of longitudinal PLS correlation analysis. **(F)** Output of PLS correlation for each significant LC. FSD, function-structure dependency; LC, latent component; PLS, partial least squares; SC, structural connectome; SDI, structural decoupling index.

participants were excluded because they were too young for clinical assessment or had missing data points. For the rest of the 100 participants with the deletion, patients were considered PPS(+) (n = 52) if they scored ≥3 during at least 1 visit on any of the subscales for PPSs. The remaining participants were considered PPS(−) (n = 48). With this clinical cutoff, we wanted to focus on which patients reach the intensity of mild to moderate psychotic symptoms. This criterion was chosen in line with studies that have shown the clinical value of this threshold for determining psychosis high-risk state (40–42). Given that the frequency and intensity of PPSs is known to fluctuate considerably across time, to characterize atypical neurodevelopmental mechanisms that may contribute vulnerability to their emergence, a score ≥3 represents a more liberal threshold, which would essentially separate individuals who endorsed psychotic symptoms at some point from those who did not.

PLS-C With Longitudinal Regressors

As illustrated in Figure 1E, F, to explore longitudinal changes in FSD maturation, we utilized PLS-C (31,43) using the myPLS toolbox (https://github.com/MIPLabCH/myPLS). Behavioral variables, including diagnosis and age regressors, were incorporated to capture brain maturation over time. Mean age, delta age, and interage constructs were defined to reflect cross-sectional, longitudinal, and interaction effects, respectively. PLS-C was applied to FSD values and age longitudinal regressors for all participants. The significance of latent components (LCs) was determined via permutation testing followed by bootstrap analysis for stability assessment. Sex and motion estimates during rs-fMRI were regressed out prior to PLS-C. Brain and development scores were derived for each participant to complement brain and behavioral saliency insights. A detailed explanation of the inputs and the procedure of the PLS-C is provided in Supplemental Methods.

RESULTS

To assess the difference between FSD development in patients with 22q11.2DS and HCs, we applied a longitudinal PLS-C analysis, which resulted in 4 significant LCs (LC1: $p < .001$, LC2: $p < .001$, LC3: $p < .002$, LC4: $p < .004$) that explained 90% of the cross-covariance. Below, we describe LCs 1 to 3 in terms of their developmental trajectories and the associated

brain regions. LC4 is discussed in the Supplement because its explained cross-covariance was <9%.

A second PLS-C analysis was conducted to compare differences among patients with and without PPSs. This assessment of FSD on PPSs resulted in 2 significant components (PPS-LCs) (PPS-LC1: $p < .001$, PPS-LC2: $p < .001$) that explained 59% of the 22q11.2DS data. Subsequently, we describe how PPS-LC1 and PPS-LC2 captured different developmental trajectories with their associated brain pattern in the 2 subgroups in the deletion carriers.

LC1: Divergence of Developmental Trajectory of FSD in 22q11.2DS

LC1 ($p = .001$) accounted for 37.76% of FSD-behavior cross-covariance (Figure S4), with a strong post hoc correlation ($r = 0.46$) between FSD values and behavioral scores (Figure 1A, B). Given the consistent increasing expression of this component in HCs, it can be interpreted as the FSD maturation pattern that patients with 22q11.2DS failed to follow. HCs showed steady maturation with age, whereas participants with 22q11.2DS expressed almost no developmental increase. Furthermore, the FSD developmental trajectory started to decrease its expression around adolescence (Figure 1C, D).

The brain pattern (Figure 1E) was characterized by 2 sets of regions that showed opposite developmental FSD alterations. The first set, displayed in blue, consisted of regions with progressive coupling in HCs but failure to increase coupling in participants with 22q11.2DS, which developed a larger gap during adolescence. Such progressive hypocoupling included regions of the frontoparietal network (left posterior parts of the temporal gyrus, left inferior parietal gyrus, medial cingulate cortex, and lateral prefrontal cortex [PFC]), the salience/ventral attention network (frontomedial lobule, inferior parietal lobule, and left insula), the default mode network (DMN) (posterior cingulate cortex, left precuneus, medial PFC), and supplementary motor regions, as well as the subcortical ventro- and dorsoposterior thalamus, right dorsoanterior thalamus, nucleus accumbens shell, left anterior caudate, and left medial amygdala. Conversely, the regions displayed in red presented a developmental excessive coupling in participants with 22q11.2DS. Such developmental hypercoupling included regions of the DMN–medial temporal lobe network (parts of the right temporal gyrus, right temporal poles, right superioparietal lobule, left fusiform, and right lateral amygdala), as well as the subcortical right anterior globus pallidus.

LC2: Early Hit in 22q11.2DS

LC2 ($p = .001$) accounted for 25.71% of FSD-behavior cross-covariance (Figure S4), with a strong post hoc correlation ($r = 0.65$) between FSD values and behavioral scores (Figure 2A).

This component was mainly characterized by a similar maturation trajectory accompanied by a negative offset, which persisted into adulthood (Figure 2C, D).

The brain pattern (Figure 2E) regions displayed in blue had generally lower coupling in 22q11.2DS, although increasing coupling with age was found in both groups. Hypocoupling in 22q11.2DS largely affected regions involved in the DMN (precuneus, parahippocampus, retrosplenial cortex, superioparietal cortex, and temporal lobe), dorsal and lateral PFC, visual cortex, and subcortical anterior putamen. Regions displayed in red consisted of regions with general hypercoupling in patients with 22q11.2DS and decreasing coupling with age in both groups. Such hypercoupling in 22q11.2DS included regions in the primary and secondary somatomotor network (motor, premotor, sensorimotor, auditory), temporal lobes, right temporal poles, orbitofrontal cortex, subcortical nucleus accumbens, and left ventroposterior thalamus.

LC3: Potential Compensation in 22q11.2DS

LC3 ($p = .002$) accounted for 18.70% of FSD-behavior cross-covariance (Figure S4), with a strong post hoc correlation ($r = 0.52$) between FSD values and behavioral scores (Figure 3A).

This component can be interpreted as one that is exclusively expressed in 22q11.2DS and reflected an overshoot as age increased. LC3 was scarcely expressed in HCs (as demonstrated by the development score remaining steadily around 0), whereas patients with 22q11.2DS showed a developmental decreasing trajectory that was largely driven by the delta age loading (Figure 3C, D).

The brain pattern (Figure 1E) regions displayed in blue were characterized by initial hypercoupling that turned into hypocoupling in 22q11.2DS. These regions are part of the left salience–ventral attention network (left inferior frontal operculum, left ventrolateral PFC, inferior parietal lobule, frontal-parietal midline regions) and the dorsal attention network (frontal eye field and posterior parietal cortex). Regions displayed in red represented an initial hypocoupling that eventually developed into a hypercoupling in 22q11.2DS. Such developmental hypercoupling mainly affected regions in the inferior temporal lobes and temporal poles, left parahippocampus, right primary and secondary somatomotor and central visual regions, auditory cortex, and insula as well as the subcortical left lateral amygdala, right anterior globus pallidus, right anterior caudate, right dorsoposterior thalamus, and ventroposterior thalamus.

Longitudinal PLS Revealed 2 Robust LCs Linking FSD With PPSs

PPS-LC1: Strong Developmental Contrast in PPS(+/−) in 22q11SD. PPS-LC1 ($p = .001$) accounted for 36.32% of FSD-behavior cross-covariance (Figure S6), with a strong post hoc correlation ($r = 0.50$) between FSD values and behavioral scores (Figure 4A).

This brain component can be interpreted as one that mainly showed an FSD developmental distinction between patients with and without PPSs. Both psychopathology and aging had a considerable effect on this component (Figure 4B), as expressed by a clear decrease in FSD maturation starting around adolescence for patients with PPSs (Figure 4C, D).

The brain pattern (Figure 4E) encompassed regions in blue with higher coupling in patients without PPSs and abnormally low coupling in patients with PPSs, which became most severe during adolescence. Such progressive hypocoupling largely included the inferior frontal gyrus, supplementary motor areas, the control network (lateral PFC and medial cingulate cortex), the salience/ventral attention network (left insula and left

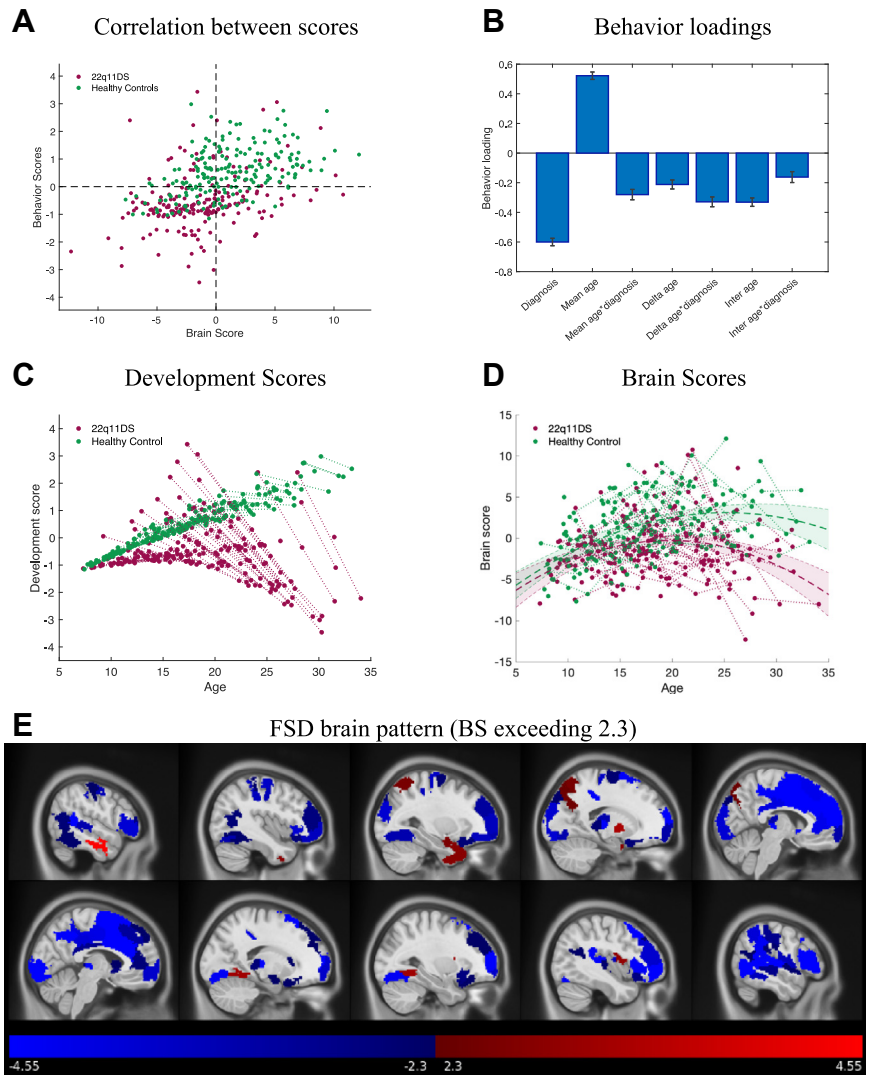

Blue: lower coupling in 22q11.2DS, failure to increase during development
Red: higher coupling in 22q11.2DS, decreasing developmental trajectory

Figure 2. Latent component 1 (LC1) showed developmental divergence in 22q11.2DS. LC1 reflected typical development and its deviation in 22q11.2DS. **(A)** Correlation between individual-specific FSD values and behavioral scores of healthy control participants (green) and patients with 22q11.2DS (purplish-red). **(B)** The design salience of LC1 revealed a negative diagnosis effect, a positive mean age effect, and a negative effect of the age × diagnosis interaction. **(C)** Comparing development scores of patients with 22q11.2DS with those of healthy control participants revealed that age scores increased with age in healthy control participants but failed to follow the development pace and even start to decrease at age 15 for patients. **(D)** BSs were lower in patients with 22q11.2DS (negative diagnosis effect). In addition, BSs were less affected by aging (negative interaction effect) in patients, which points toward dysmaturation. Fitted line and 95% CIs are plotted to visualize the age × diagnosis interaction effect captured by partial least squares correlation in the bar plot in **(B)**. **(E)** The pattern of brain salience can be interpreted as areas of developmental too low coupling (blue) and developmental too high coupling (red) in patients with 22q11.2DS. Slice direction from top left to bottom right: from the right to the left side of the brain. 22q11.2DS, 22q11.2 deletion syndrome; BS, brain score; FSD, function-structure dependency.

inferior parietal lobule), and the DMN (right anterior and posterior cingulate cortices, precuneus, and right medial PFC). The regions presented in red showed developmental excessive coupling in patients with PPSs. Such developmental hypercoupling largely included regions of the inferior temporal gyrus, temporal poles, right insula, left orbitofrontal cortex, and exclusively right subcortical structures (ventroanterior thalamus, nucleus accumbens core, anterior globus pallidus, and anterior caudate).

PPS-LC2: Maturation of 22q11.2DS Carriers. PPS-LC2 (p = .001) accounted for 22.62% of FSD-behavior cross-covariance (Figure S6), with a large post hoc correlation (r = 0.64) between FSD values and behavioral scores (Figure 5A).

This component mainly captured the effect of maturation as indicated by an effect for diagnosis and a stronger effect for aging as indicated by a large stable mean age loading (Figure 5C, D).

The brain pattern (Figure 5E) regions displayed in blue showed higher coupling in patients with PPSs and increasing coupling with age in both groups. Developmental hypercoupling affected parts of the superior parietal lobule, insula, lateral PFC, and right precuneus. Regions in red had lower coupling in patients with PPSs and decreasing coupling with age in both groups. Such hypocoupling was present in regions of the visual network (striate and extrastriate), paracentral lobule, medial cingulate, subcortical bilateral nucleus accumbens shell, anterior caudate, and left posterior hippocampus.

DISCUSSION

We employed a multivariate longitudinal analysis to explore FSD across the brain in a substantial cohort of individuals with 22q11.2DS and provided robust evidence of abnormal FSD development. Two distinct developmental patterns emerged:

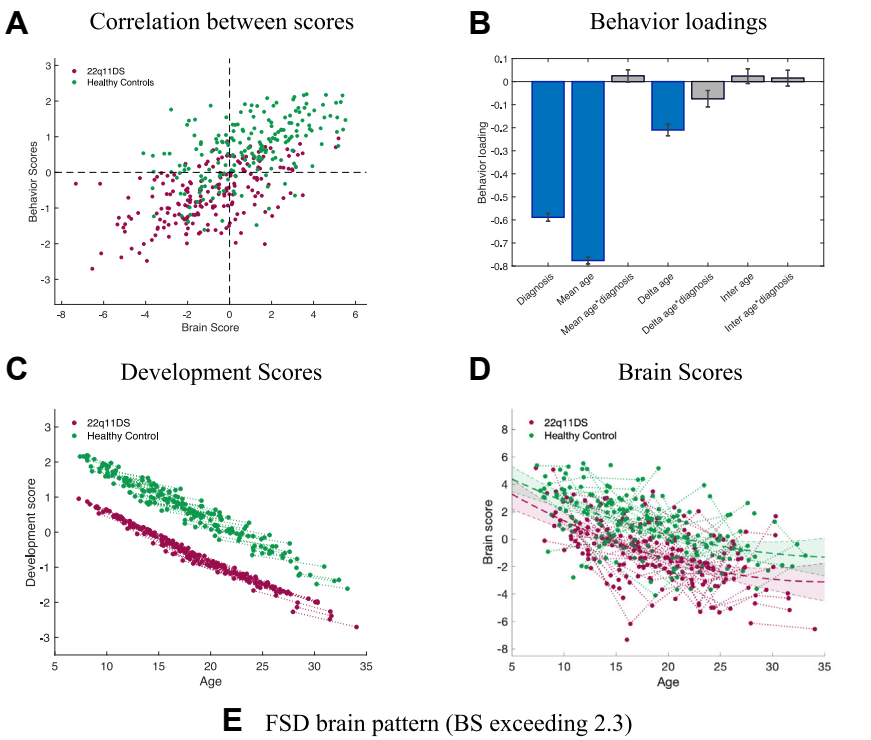

Figure 3. Latent component 2 (LC2) showed early offset in 22q11.2DS. LC2 reflected an early hit. **(A)** Correlation between individual-specific FSD values and behavioral scores of healthy control participants (green) and patients with 22q11.2DS (purplish-red). **(B)** The design salience of LC2 revealed a large negative diagnosis and a negative mean age effect. **(C)** Comparing developmental scores of patients with 22q11.2DS with those of healthy control participants revealed a negative offset that was already present at the beginning of the age span (7 years) and persisted throughout development. **(D)** BSs were lower in patients with 22q11.2DS (negative diagnosis effect), but both patients with 22q11.2DS and healthy control participants showed a developmental decrease with increasing age. Fitted line and 95% CIs are plotted to visualize the age × diagnosis interaction effect captured by partial least squares correlation in the bar plot in **(B)**. **(E)** The pattern of brain salience can be interpreted as areas of developmental too low coupling (blue) and developmental too high coupling (red) in patients with 22q11.2DS. However, the negative slope has to be interpreted as an increase in coupling strength. 22q11.2DS, 22q11.2 deletion syndrome; BS, brain score; FSD, function-structure dependency; LC, latent component.

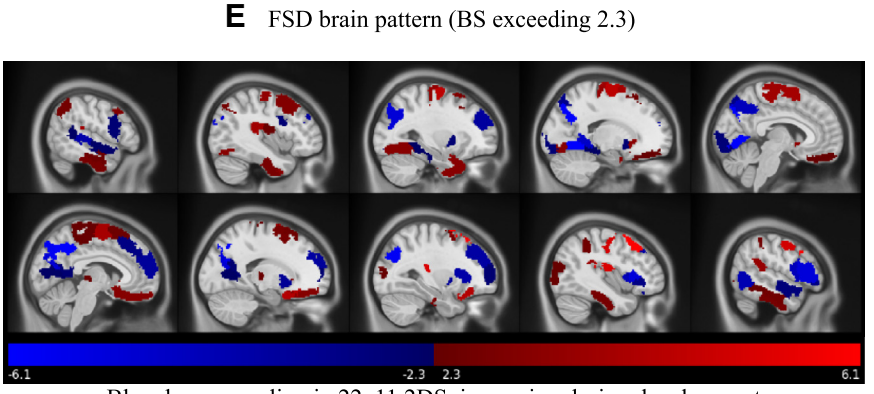

Blue: hypo-coupling in 22q11.2DS, increasing during development
Red: hyper-coupling in 22q11.2DS, decreasing developmental trajectory

an early hit, manifested by a shift in FSD that persisted throughout development, and an exacerbation of FSD deviation that occurred during adolescence and was associated with the emergence of PPSs.

Early Hit Persisted Throughout Development: Implication for Overall Deficits in 22q11.2DS

LC2 (Figure 2C) shows participants with 22q11.2DS displaying an early FSD developmental offset that persisted throughout their development. This offset implies an equivalent 5- to 7-year delay in brain development between HCs and individuals with 22q11.2DS, which suggests the possibility of a developmental FSD deviation in 22q11.2DS that begins early in life. Looking at the brain pattern of LC2 (Figure 2E), this delay affected regions involved in higher-order cognitive, behavioral, and motor coordination–related regions—all categories well known as difficulties in participants with 22q11.2DS (44–46).

Notably, PPS-LC2 exhibited a similar age pattern as LC2 (Figure 6B–D), which indicates that the sustained deviation in LC2 is not only a distinguishing factor between HCs and individuals with 22q11.2DS but also contains information related to PPSs, which is represented as a slight gradient among PPS(+/−) patients (Figure 6A, C, D). Surprisingly, patients with PPS(+) demonstrated a brain pattern slightly more closely aligned with HCs than PPS(−) patients, indicating that other factors such as neurobiological or environmental influences play a more substantial role in the emergence of PPSs than the FSD deviations captured in PPS-LC2. Furthermore, this may reveal a compensatory brain development mechanism in

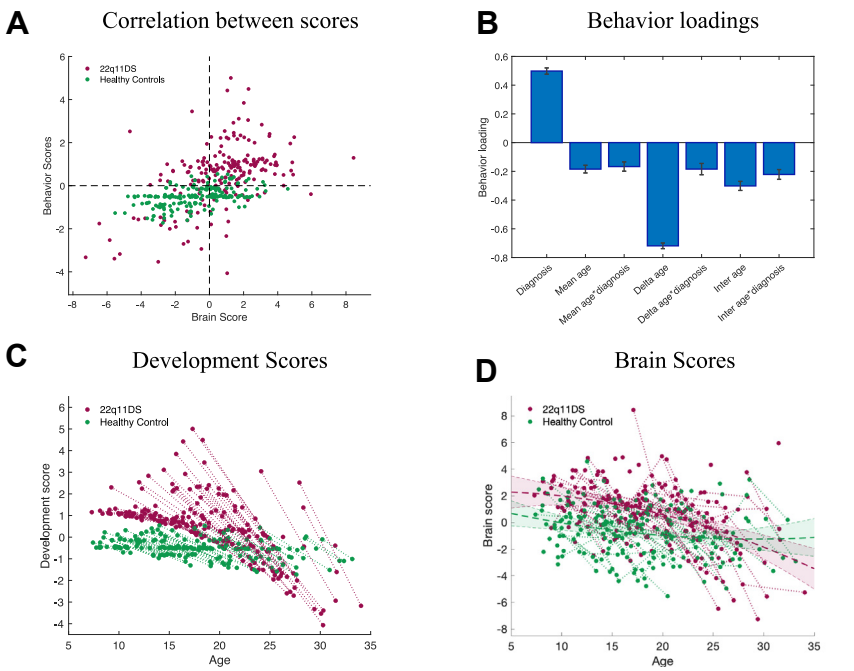

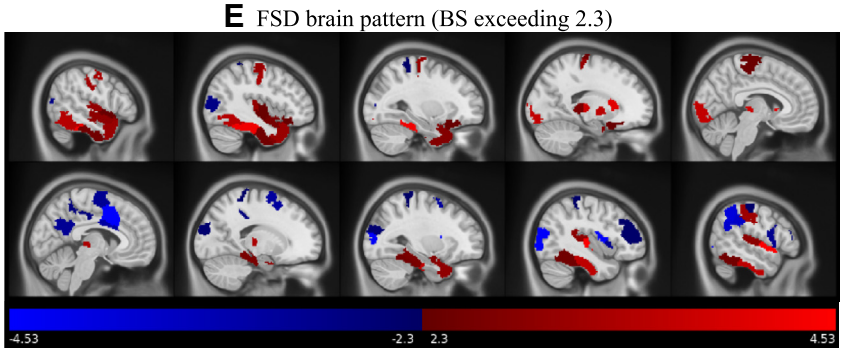

Blue: hyper- coupling in 22q11.2DS, decreasing trajectory until hypo-coupling in 22q11.2DS

Red: hypo-coupling in 22q11.2DS, increasing trajectory until hyper-coupling in 22q11.2DS

Figure 4. Latent component 3 (LC3) showed a late overshoot in 22q11.2DS. LC3 reflected an overcompensation in 22q11.2DS. **(A)** Correlation between individual-specific FSD values and behavioral scores of healthy control participants (green) and patients with 22q11.2DS (purplish-red). **(B)** The design salience of LC3 revealed a positive diagnosis effect as well as a negative effect of the age × diagnosis interaction. **(C)** Comparing development scores of patients with 22q11.2DS with those of healthy control participants revealed that age scores decreased longitudinally in healthy control participants and patients but started to decrease even more strongly at age 15 in patients. **(D)** BSs were initially higher in patients with 22q11.2DS (positive diagnosis effect), but values during adulthood were lower (negative age effects). Fitted line and 95% CIs are plotted to visualize the age × diagnosis interaction effect captured by partial least squares correlation in the bar plot in **(B)**. **(E)** The pattern of brain salience can be interpreted as areas of initially too high coupling (blue) and too low coupling (red) in patients that developed progressively into too low coupling (blue) and too high coupling (red) in patients with 22q11.2DS. Slice direction from top left to bottom right: from the right to the left side of the brain. 22q11.2DS, 22q11.2 deletion syndrome; BS, brain score; FSD, function-structure dependency.

22q11.2DS. Such compensatory mechanisms have been documented in schizophrenia, where changes in brain structure and function appear as deviations from healthy norms but are associated with less severe symptoms and better cognitive profiles (47,48). In this situation, genetically susceptible regions may have potentially localized compensatory changes to escape the negative influence of the disease risk on its structure and function. Thus, increased local deviations of regions visible in Figure 6 (PPS-LC2) may be interpreted as compensatory processes that lead to less severe psychotic symptoms in patients with 22q11.2DS. This tentative explanation should be taken with caution, and more investigation is needed to elucidate the impact of the early hit on compensatory mechanisms in psychotic symptoms. In conclusion, the early hit comes with a persistent offset that does not appear to cause the occurrence of PPSs but may contribute to day-to-day difficulties experienced by deletion carriers.

Abnormal FSD Was Aggravated During Adolescence: A Central Feature in 22q11.2DS and Psychotic Symptoms

Both LC1 (Figure 1C) and LC3 (Figure 3C) revealed a developmental exacerbation of abnormal FSD during adolescence in 22q11.2DS. LC1 demonstrated less coupling, primarily in the frontal and cingulate cortices, while LC3 exhibited increased coupling in the temporal cortices, regions well known for their involvement in higher-order cognitive functions (49–52). This relationship was recently further confirmed in a study investigating individual cognition and SDI. The authors showed that better cognition prediction was achieved by using high-level hierarchical SDI brain regions such as the PFC (53). Interestingly, executive function has been associated with lower prefrontal SDI (54). These findings suggest that although hierarchically higher SDI brain regions are significantly involved in cognition, optimal cognitive performance does not

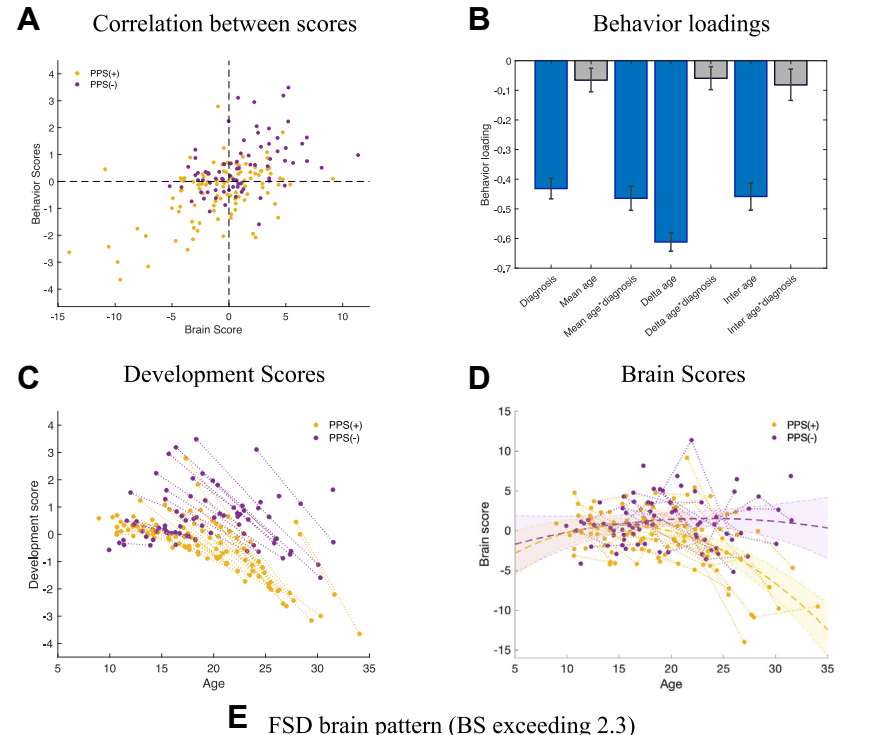

Figure 5. The fourth latent component (PPS-LC1) showed developmental divergence in PPS(+). PPS-LC1 reflected a FSD development distinction in PPS(+) and PPS(–) patients. **(A)** Correlation between individual-specific FSD values and behavioral scores of PPS(−) (blue) and PPS(+) participants (orange). **(B)** Design salience of PPS-LC1 revealed exclusively negative diagnosis and negative age effects. **(C)** Comparing PPS(+) vs. PPS(−) patients revealed that the longitudinal decrease in age scores became more severe in PPS(+) patients during adolescence. **(D)** The distribution of BSs across age in each group showed that FSD development in PPS(+) patients decreased further from that in PPS(–) patients during adolescence. Fitted line and 95% CIs are plotted to visualize the age × diagnosis interaction effect captured by partial least squares correlation in the bar plot in **(B)**. **(E)** The pattern of brain salience can be interpreted as areas of developmental lower coupling (blue) and developmental higher coupling (red) in PPS(+) patients. Slice direction from top left to bottom right: from the right to the left side of the brain. BS, brain score; FSD, function-structure dependency; LC, latent component; PPS, positive psychotic symptom.

Blue: hypo-coupling in PPS(+), failure to increase during development
Red: hyper-coupling in PPS(+), decreasing developmental trajectory

necessarily correlate with an increasing degree of decoupling. Our findings in LC1, showing abnormally lower coupling (higher SDI) in frontal regions in patients, suggest that too low coupling (too high SDI) may also not be conducive to optimal cognitive function. This implies the existence of a locally nuanced FSD bandwidth within which healthy brain performance thrives. Notably, LC1 mirrors results from a previous cross-sectional study that compared coupling strength in adults with and without 22q11.2DS (7) (see Figure S11 for quantification of the similarity of whole-brain FSD values). Therefore, LC1 may present the developmental pathway that leads to the impairment found in adults. Moreover, LC1 is primarily driven by normal maturation of the healthy population (see Figures S13 and S16 for separate group PLS-C). This may lend evidence to previous conjecture (7) that optimal frontal FSD is partially a result of the pruning process of structural connections that occur in typical development. We observed patients with 22q11.2DS exhibiting abnormally lower coupling in frontal regions. Increasing evidence suggests abnormal pruning processes that contribute to an immature frontal cortex struggling to establish optimal connections to support complex executive functions (30,55). Structural impairments in the PFC and abnormal pruning have been documented in 22q11.2DS (56,57). A recent mouse study documented the crucial role of glutamate in synaptic pruning, where glutamate binds to NMDA receptors and thereby protects dendrites from being pruned (58). Interestingly, the very recent study mentioned above (53) reported a significant relationship between higher SDI and higher glutamate (mGluR5) receptors/transporters predominantly in frontal regions. Elevated glutamatergic levels in the PFC, including the anterior cingulate cortex, were observed in unmedicated patients with

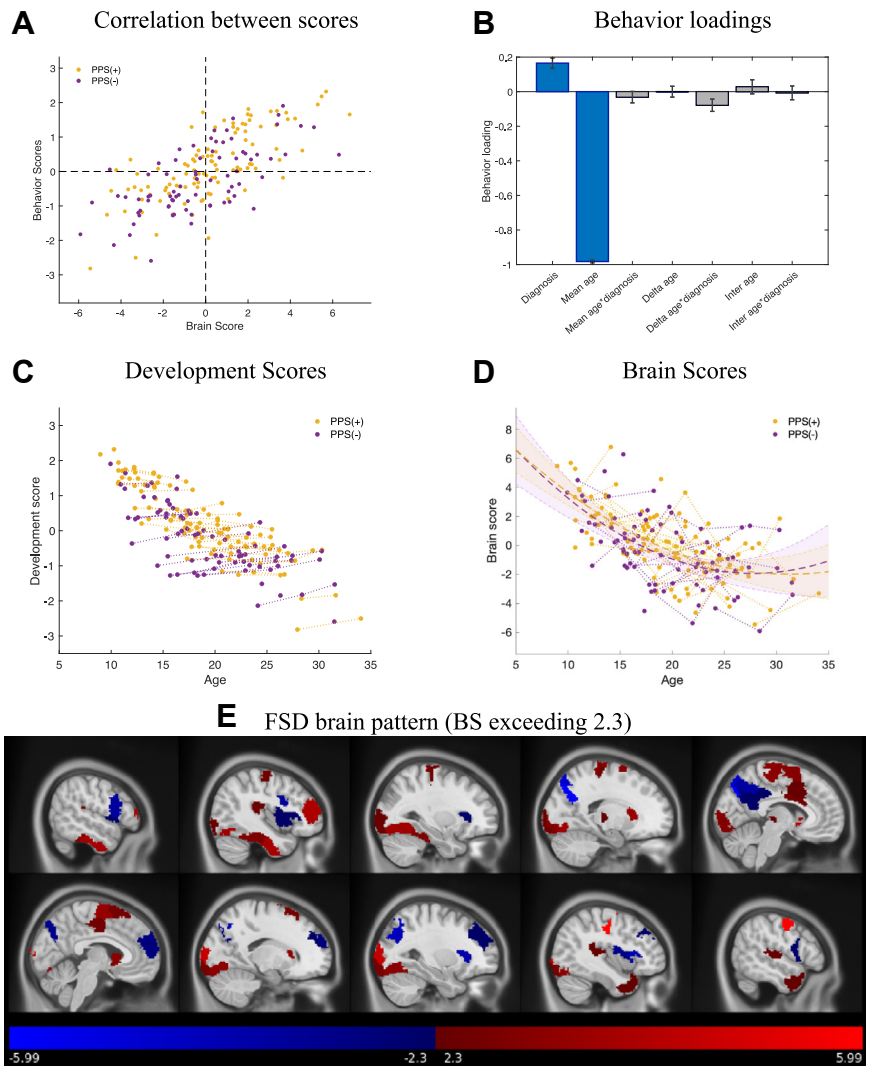

Blue: hyper-coupling in PPS(+), decreasing developmental trajectory
Red: hypo-coupling in PPS(+), increasing during development

Figure 6. PPS-LC2 showed the maturation of deletion carriers. The fifth latent component (PPS-LC2) reflected a gradient PPS(+) and PPS(–) patients. **(A)** Correlation between individual-specific FSD values and behavioral scores of PPS(−) (blue) and PPS(+) (orange) participants. **(B)** The design salience of LC2 revealed a positive diagnosis and a large negative mean age effect. **(C)** Comparing developmental scores of PPS(+) patients to those of PPS(−) patients revealed a negative development for both groups, with a slight offset persisting throughout development. **(D)** BSs were slightly higher in PPS(+) patients (positive diagnosis effect). Fitted line and 95% CIs are plotted to visualize the age × diagnosis interaction effect captured by partial least squares correlation in the bar plot in **(B)**. **(E)** The pattern of brain salience can be interpreted as areas of developmental higher coupling (blue) and developmental lower coupling (red) in PPS(+) patients. However, the negative slope has to be interpreted as an increase in coupling strength (blue) as well as decreasing coupling strength (red) for both groups. Slice direction from top left to bottom right: from the right to the left side of the brain. BS, brain score; FSD, function-structure dependency; LC, latent component; PPS, positive psychotic symptom.

schizophrenia (59–61) and in patients with 22q11.2DS (62). Although our results do not present any direct link to glutamatergic levels or pruning processes, our findings and the literature support the link between abnormal FSD development and abnormal pruning processes possibly caused by disturbed glutamatergic signaling in patients with 22q11.2DS. However, the underlying mechanism behind the abnormal high coupling in temporal regions is not clear and requires further investigation.

Interestingly, our findings in patients with and without mild to moderate PPSs revealed a similar onset of alterations during adolescence and brain pattern (Figure 4D, E) as LC1. Notably, the alteration was predominantly driven by patients with PPSs. The parallel contrasts observed in both HCs/22q11.2DS (LC1) and PPS(+/−) (PPS-LC1) patients underscore the documented notion of psychosis as a consequence of atypical adolescent brain maturation (63–65). Hypocoupling was observed in core regions of the DMN (precuneus–posterior cingulate cortex, anterior cingulate cortex–medial PFC) and in task-positive regions (lateral PFC, supplementary motor region, right inferior parietal lobule, left insula, and left auditory cortex). With respect to hypercoupling, only the inferior temporal gyrus, temporal poles [as sensory-associated nodes of the DMN (66–68)], and parts of the striatum were revealed. DMN-related functions appear to be altered in patients expressing PPSs (69–73), with recent studies on psychotic symptoms demonstrating that patients with schizophrenia fail to reduce DMN activity during task performance (74–76). This suggests that efficient DMN suppression during externally goal-directed cognitive tasks is crucial for adaptive disengagement from internal information processing (77). Impaired DMN suppression may hinder individuals from focusing on

ongoing tasks (78,79). The presence of abnormally low coupling in core DMN nodes and task-positive regions may indicate a deficit in functional segregation between these networks (80,81). This deficit may result from insufficient differentiation of functional processes despite underlying structural connections (82). On the other hand, previous studies have linked increased coupling to more direct control of cortical regions by sensory inputs (83,84). Therefore, excessive coupling in sensory-associated DMN nodes and in the striatum may reflect overengagement in activation. This overactivation may result in simultaneous activation of the DMN and task-related networks even when one should be deactivated, which causes a blending of intrinsic and extrinsic information processing. In fact, abnormal coactivation of the DMN with sensory thalamic loops has been documented in patients with 22q11.2DS and proposed as a mechanism of sensory hallucinations (85,86). Moreover, studies have shown that altered dynamics of activation and deactivation between the DMN and task-positive networks leads to concurrent activation, thereby attenuating the intended brain signals (87,88). Therefore, excessive coupling of sensory DMN and striatum may lead to misattributed salience, potentially blurring the distinction between one's internal mental and external reality and thus contributing to the manifestation of abnormal perceptions and delusional experiences (89).

Conclusion and Future Perspectives

We examined healthy and abnormal maturation of whole-brain FSD in neurotypical control individuals and patients with 22q11.2DS using FSD in a multivariate longitudinal analysis. This study provides the first evidence of altered developmental trajectories in 22q11.2DS across a whole-brain FSD pattern. However, the findings of this study prompt some methodological considerations. While multivariate longitudinal analysis is a powerful tool for detecting abnormal patterns undergoing development, these patterns must be considered as a whole, and no strict conclusions can be drawn for the individual nodes. The studied population is a mixture of longitudinal and cross-sectional samples. Acquiring high-quality longitudinal data from patients with a rare deletion is extremely challenging, and this cohort is unique in this regard. In this respect, the flexibility of the longitudinal PLS-C to adapt the number of visits for each participant makes it particularly well equipped to consider the combination of longitudinal and cross-sectional data. Furthermore, tractography reconstruction was applied on diffusion tensors obtained from single-shell dMRI images acquired along 30 directions using a b value of 1000 s/mm, which are the minimal technical requirements for optimal tensor estimation (90). To compensate for that, anatomically constrained tractography and spherical deconvolution–informed filtering of tractograms algorithms were adopted in the tractographic reconstruction of the structural connectome. These methods have been shown to produce more biologically realistic connectomes (91,92), leading to more interpretable results. Nonetheless, this correction is not perfect, and brain network metrics computed on structural connectome were previously shown to be affected by the methods used to perform tractogram bias correction (93). The effect of different structural connectome processing choices may need evaluation in future work. Additionally, considering medication and its potential confounding effects was difficult because this large, long-term ongoing cohort accepts participants treated by multiple physicians. Therefore, obtaining a comprehensive history of medication input along with dosage and control of the adherence to the treatment is difficult. The same is also valid for the information of the deletion breakpoint subtypes. There was not precise enough information from deletion carriers to consider it in our analysis. For a thorough evaluation of the effect of medication or deletion breakpoint subtypes on FSD alterations, a more controlled setting is needed.

This is the first study to assess longitudinal FSD alterations and their contribution to psychopathology in 22q11.2DS. Our work has identified 2 distinct FSD development patterns in this population. The first pattern indicated an early onset alteration, reflecting a persistent gap between HCs and individuals with 22q11.2DS and signifying a delay in brain development. The brain regions affected by this early hit match the wide range of behavioral and cognitive deficits that have been reported in the literature on 22q11.2DS. The second pattern showed a clear developmental deviation that is exacerbated during adolescence, which affects brain regions with both hyper- and hypocoupling compared with HCs. This FSD deviation severity appears to be linked to a higher risk of developing psychotic symptoms.

These findings confirm that the analysis of longitudinal FSD data can pinpoint neural substrates despite the broad variability in behavior and psychopathological development seen in 22q11.2DS. Due to the still sparse literature on FSD and particularly its biological underpinning, future studies are needed to provide further insight into the biological correlates of FSD, such as microstructural changes (e.g., multi-shell diffusion), further investigation of neurotransmitter concentrations like dopamine or glutamate (e.g., magnetic resonance spectroscopy), the dynamics between and within brain networks (e.g., coactivation pattern analysis), or even translational studies (e.g., in mice) that combine fMRI with invasive measures of brain structure. These additional measures may help us understand the mechanisms that underlie developmental FSD changes.

ACKNOWLEDGMENTS AND DISCLOSURES

This work was supported by the Swiss National Science Foundation (Grant Nos. 324730_121996 and 324730_144260 [to SE]) and the National Centre of Competence in Research Synapsy (Grant No. 51NF40-158776 [to SE]).

SF, FD, CS, HR, MGP, DVDV, and SE were responsible for conceptualization. SF, FD, and SE were responsible for investigation. SF, FD, MGP, and DVDV developed the methodology. SF and FD were responsible for formal analysis. SF, FD, and MGP were responsible software. SF, FD, and HR were responsible for writing the original draft of the manuscript. SF and FD were responsible for visualization. CS, DVDV, and SE were responsible for conceptualization and reviewing and editing the manuscript. DVDV and SE were responsible for resources, supervision, project administration, and funding acquisition.

We are grateful to all the families who participated in our study and thank Tereza Kotalova for coordinating the project and the MRI scanner operators at the Centre d'Imagerie BioMédicale, Pamela Charpilloz, Tania Rappo, and Greta Moltrasio, for their help during data collection.

The authors report no biomedical financial interests or potential conflicts of interest.

ARTICLE INFORMATION

From the Developmental Imaging and Psychopathology Laboratory, University of Geneva School of Medicine, Geneva, Switzerland (SF, FD, CS, HR, SE); Medical Image Processing Laboratory, Neuro-X Institute, École Polytechnique Fédérale de Lausanne, Lausanne, Switzerland (SF, FD, MGP, DVDV); Developmental Clinical Psychology Research Unit, University of Geneva Faculty of Psychology and Educational Sciences, Geneva, Switzerland (HR); Department of Radiology and Medical Informatics, University of Geneva, Geneva, Switzerland (MGP, DVDV); CIBM Center for Biomedical Imaging, Lausanne, Switzerland (MGP, DVDV); and the Department of Genetic Medicine and Development, University of Geneva School of Medicine, Geneva, Switzerland (SE).

Address correspondence to Silas Forrer, M.B.E., at silas.forrer@unige.ch.

Received Jan 3, 2024; revised May 3, 2024; accepted May 19, 2024.

Supplementary material cited in this article is available online at https://doi.org/10.1016/j.bpsc.2024.05.008.

REFERENCES

1. Fox MD, Snyder AZ, Vincent JL, Corbetta M, Van Essen DC, Raichle ME (2005): The human brain is intrinsically organized into dynamic, anticorrelated functional networks. Proc Natl Acad Sci USA 102:9673–9678.
2. Bressler SL, Menon V (2010): Large-scale brain networks in cognition: Emerging methods and principles. Trends Cogn Sci 14:277–290.
3. Filley CM, Fields RD (2016): White matter and cognition: Making the connection. J Neurophysiol 116:2093–2104.
4. Sporns O (2013): Structure and function of complex brain networks. Dialogues Clin Neurosci 15:247–262.
5. Becker CO, Pequito S, Pappas GJ, Miller MB, Grafton ST, Bassett DS, Preciado VM (2018): Spectral mapping of brain functional connectivity from diffusion imaging. Sci Rep 8:1411–1411.
6. Preti MG, Van De Ville D (2019): Decoupling of brain function from structure reveals regional behavioral specialization in humans. Nat Commun 10:4747.
7. Bortolin K, Delavari F, Preti MG, Sandini C, Mancini V, Mullier E, *et al.* (2022): Neural substrates of psychosis revealed by altered dependencies between brain activity and white-matter architecture in individuals with 22q11 deletion syndrome. NeuroImage Clin 35:103075.
8. Sydnor VJ, Larsen B, Seidlitz J, Adebimpe A, Alexander-Bloch AF, Bassett DS, *et al.* (2023): Intrinsic activity development unfolds along a sensorimotor–association cortical axis in youth. Nat Neurosci 26:638–649.
9. Johnson MH (2001): Functional brain development in humans. Nat Rev Neurosci 2:475–483.
10. Segal A, Parkes L, Aquino K, Kia SM, Wolfers T, Franke B, *et al.* (2023): Regional, circuit and network heterogeneity of brain abnormalities in psychiatric disorders. Nat Neurosci 26:1613–1629.
11. Lawrie SM, Buechel C, Whalley HC, Frith CD, Friston KJ, Johnstone EC (2002): Reduced frontotemporal functional connectivity in schizophrenia associated with auditory hallucinations. Biol Psychiatry 51:1008–1011.
12. Karbasforoushan H, Woodward ND (2012): Resting-state networks in schizophrenia. Curr Top Med Chem 12:2404–2414.
13. Hoptman MJ, Nierenberg J, Bertisch HC, Catalano D, Ardekani BA, Branch CA, Delisi LE (2008): A DTI study of white matter microstructure in individuals at high genetic risk for schizophrenia. Schizophr Res 106:115–124.
14. Camchong J, Lim KO, Sponheim SR, MacDonald AW (2009): Frontal white matter integrity as an endophenotype for schizophrenia: Diffusion tensor imaging in monozygotic twins and patients' nonpsychotic relatives. Front Hum Neurosci 3:35–35.
15. Griffa A, Baumann PS, Klauser P, Mullier E, Cleusix M, Jenni R, *et al.* (2019): Brain connectivity alterations in early psychosis: From clinical to neuroimaging staging. Transl Psychiatry 9:62–62.
16. Schilbach L, Hoffstaedter F, Müller V, Cieslik EC, Goya-Maldonado R, Trost S, *et al.* (2016): Transdiagnostic commonalities and differences in resting state functional connectivity of the default mode network in schizophrenia and major depression. NeuroImage Clin 10:326–335.
17. Padula MC, Schaer M, Scariati E, Schneider M, Van De Ville D, Debbané M, Eliez S (2015): Structural and functional connectivity in the default mode network in 22q11.2 deletion syndrome. J Neurodev Disord 7:23–23.
18. Matsuo K, Chen SHA, Liu CM, Liu CC, Hwang TJ, Hsieh MH, *et al.* (2013): Stable signatures of schizophrenia in the cortical-subcortical-cerebellar network using fMRI of verbal working memory. Schizophr Res 151:133–140.
19. Giraldo-Chica M, Woodward ND (2017): Review of thalamocortical resting-state fMRI studies in schizophrenia. Schizophr Res 180:58–63.
20. Hermundstad AM, Bassett DS, Brown KS, Aminoff EM, Clewett D, Freeman S, *et al.* (2013): Structural foundations of resting-state and task-based functional connectivity in the human brain. Proc Natl Acad Sci USA 110:6169–6174.
21. Stiso J, Bassett DS (2018): Spatial embedding imposes constraints on neuronal network architectures. Trends Cogn Sci 22:1127–1142.
22. Biswas AB, Furniss F (2016): Cognitive phenotype and psychiatric disorder in 22q11.2 deletion syndrome: A review. Res Dev Disabil 53–54:242–257.
23. Lewandowski KE, Shashi V, Berry PM, Kwapil TR (2007): Schizophrenic-like neurocognitive deficits in children and adolescents with 22q11 deletion syndrome. Am J Med Genet B Neuropsychiatr Genet 144B:27–36.
24. Schneider M, Debbané M, Bassett AS, Chow EWC, Fung WLA, van den Bree M, *et al.* (2014): Psychiatric disorders from childhood to adulthood in 22q11.2 deletion syndrome: Results from the International Consortium on Brain and Behavior in 22q11.2 Deletion Syndrome. Am J Psychiatry 171:627–639.
25. Schneider M, Schaer M, Mutlu AK, Menghetti S, Glaser B, Debbané M, Eliez S (2014): Clinical and cognitive risk factors for psychotic symptoms in 22q11.2 deletion syndrome: A transversal and longitudinal approach. Eur Child Adolesc Psychiatry 23:425–436.
26. McDonald-McGinn DM, Sullivan KE, Marino B, Philip N, Swillen A, Vorstman JAS, *et al.* (2015): 22q11.2 deletion syndrome. Nat Rev Dis Primers 1:15071.
27. Insel TR (2010): Rethinking schizophrenia. Nature 468:187–193.
28. Lewis DA, Levitt P (2002): Schizophrenia as a disorder of neurodevelopment. Annu Rev Neurosci 25:409–432.
29. Gomes FV, Rincón-Cortés M, Grace AA (2016): Adolescence as a period of vulnerability and intervention in schizophrenia: Insights from the MAM model. Neurosci Biobehav Rev 70:260–270.
30. Paus T, Keshavan MS, Giedd JN (2008): Why do many psychiatric disorders emerge during adolescence. Nat Rev Neurosci 9:947–957.
31. McIntosh AR, Lobaugh NJ (2004): Partial least squares analysis of neuroimaging data: Applications and advances. Neuroimage 23(suppl 1):S250–S263.
32. Scariati E, Schaer M, Richiardi J, Schneider M, Debbané M, Van De Ville D, Eliez S (2014): Identifying 22q11.2 deletion syndrome and psychosis using resting-state connectivity patterns. Brain Topogr 27:808–821.
33. Mattiaccio LM, Coman IL, Thompson CA, Fremont WP, Antshel KM, Kates WR (2018): Frontal dysconnectivity in 22q11.2 deletion syndrome: An atlas-based functional connectivity analysis. Behav Brain Funct 14:2–2.
34. Schaefer A, Kong R, Gordon EM, Laumann TO, Zuo XN, Holmes AJ, *et al.* (2018): Local-global parcellation of the human cerebral cortex from intrinsic functional connectivity MRI. Cereb Cortex 28:3095–3114.
35. Tian Y, Margulies DS, Breakspear M, Zalesky A (2020): Topographic organization of the human subcortex unveiled with functional connectivity gradients. Nat Neurosci 23:1421–1432.
36. Tournier J-D, Smith R, Raffelt D, Tabbara R, Dhollander T, Pietsch M, *et al.* (2019): MRtrix3: A fast, flexible and open software framework for medical image processing and visualisation. NeuroImage 202:116137.
37. Jenkinson M, Beckmann CF, Behrens TEJ, Woolrich MW, Smith SM (2012): FSL. NeuroImage 62:782–790.
38. Miller TJ, McGlashan TH, Rosen JL, Cadenhead K, Cannon T, Ventura J, *et al.* (2003): Prodromal assessment with the structured

interview for prodromal syndromes and the scale of prodromal symptoms: Predictive validity, interrater reliability, and training to reliability. Schizophr Bull 29:703–715.
39. Tang SX, Yi JJ, Moore TM, Calkins ME, Kohler CG, Whinna DA, *et al.* (2014): Subthreshold psychotic symptoms in 22q11.2 deletion syndrome. J Am Acad Child Adolesc Psychiatry 53:991–1000.e2.
40. Fusar-Poli P, Borgwardt S, Bechdolf A, Addington J, Riecher-Rössler A, Schultze-Lutter F, *et al.* (2013): The psychosis high-risk state: A comprehensive state-of-the-art review. JAMA Psychiatry 70:107–120.
41. Schneider M, Armando M, Pontillo M, Vicari S, Debbané M, Schultze-Lutter F, Eliez S (2016): Ultra high risk status and transition to psychosis in 22q11.2 deletion syndrome. World Psychiatry 15:259–265.
42. Mancini V, Sandini C, Padula MC, Zöller D, Schneider M, Schaer M, Eliez S (2020): Positive psychotic symptoms are associated with divergent developmental trajectories of hippocampal volume during late adolescence in patients with 22q11DS. Mol Psychiatry 25:2844–2859.
43. Krishnan A, Williams LJ, McIntosh AR, Abdi H (2011): Partial Least Squares (PLS) methods for neuroimaging: A tutorial and review. NeuroImage 56:455–475.
44. Maeder J, Schneider M, Bostelmann M, Debbané M, Glaser B, Menghetti S, *et al.* (2016): Developmental trajectories of executive functions in 22q11.2 deletion syndrome. J Neurodev Disord 8:10–10.
45. Woodin M, Wang PP, Aleman D, McDonald-McGinn D, Zackai E, Moss E (2001): Neuropsychological profile of children and adolescents with the 22q11.2 microdeletion. Genet Med 3:34–39.
46. Cunningham AC, Fung W, Massey TH, Hall J, Owen MJ, van den Bree MBM, Peall KJ (2020): Movement disorder phenotypes in children with 22q11.2 deletion syndrome. Mov Disord 35:1272–1274.
47. de Wit S, Wierenga LM, Oranje B, Ziermans TB, Schothorst PF, van Engeland H, *et al.* (2016): Brain development in adolescents at ultra-high risk for psychosis: Longitudinal changes related to resilience. NeuroImage Clin 12:542–549.
48. Palaniyappan L (2023): Clusters of psychosis: Compensation as a contributor to the heterogeneity of schizophrenia. J Psychiatry Neurosci 48:E325–E329.
49. Miller EK, Cohen JD (2001): An integrative theory of prefrontal cortex function. Annu Rev Neurosci 24:167–202.
50. Gasquoine PG (2013): Localization of function in anterior cingulate cortex: From psychosurgery to functional neuroimaging. Neurosci Biobehav Rev 37:340–348.
51. Axmacher N, Schmitz DP, Wagner T, Elger CE, Fell J (2008): Interactions between medial temporal lobe, prefrontal cortex, and inferior temporal regions during visual working memory: A combined intracranial EEG and functional magnetic resonance imaging study. J Neurosci 28:7304–7312.
52. Herlin B, Navarro V, Dupont S (2021): The temporal pole: From anatomy to function-A literature appraisal. J Chem Neuroanat 113: 101925–101925.
53. Dong X, Li Q, Wang X, He Y, Zeng D, Chu L, *et al.* (2024): How brain structure–function decoupling supports individual cognition and its molecular mechanism. Hum Brain Mapp 45:e26575.
54. Medaglia JD, Huang W, Karuza EA, Kelkar A, Thompson-Schill SL, Ribeiro A, Bassett DS (2018): Functional alignment with anatomical networks is associated with cognitive flexibility. Nat Hum Behav 2:156–164.
55. Feinberg I (1982-1983): Schizophrenia: Caused by a fault in programmed synaptic elimination during adolescence? J Psychiatr Res 17:319–334.
56. Radoeva PD, Coman IL, Antshel KM, Fremont W, McCarthy CS, Kotkar A, *et al.* (2012): Atlas-based white matter analysis in individuals with velo-cardio-facial syndrome (22q11.2 deletion syndrome) and unaffected siblings. Behav Brain Funct 8:38–38.
57. Shashi V, Veerapandiyan A, Keshavan MS, Zapadka M, Schoch K, Kwapil TR, *et al.* (2012): Altered development of the dorsolateral prefrontal cortex in chromosome 22q11.2 deletion syndrome: An in vivo proton spectroscopy study. Biol Psychiatry 72:684–691.
58. Fujimoto S, Leiwe MN, Aihara S, Sakaguchi R, Muroyama Y, Kobayakawa R, *et al.* (2023): Activity-dependent local protection and lateral inhibition control synaptic competition in developing mitral cells in mice. Dev Cell 58:1221–1236.e7.
59. Bartha R, Williamson PC, Drost DJ, Malla A, Carr TJ, Cortese L, *et al.* (1997): Measurement of glutamate and glutamine in the medial prefrontal cortex of never-treated schizophrenic patients and healthy controls by proton magnetic resonance spectroscopy. Arch Gen Psychiatry 54:959–965.
60. Théberge J, Bartha R, Drost DJ, Menon RS, Malla A, Takhar J, *et al.* (2002): Glutamate and glutamine measured with 4.0 T proton MRS in never-treated patients with schizophrenia and healthy volunteers. Am J Psychiatry 159:1944–1946.
61. Théberge J, Williamson KE, Aoyama N, Drost DJ, Manchanda R, Malla AK, *et al.* (2007): Longitudinal grey-matter and glutamatergic losses in first-episode schizophrenia. Br J Psychiatry 191:325–334.
62. Evers LJM, van Amelsvoort TAMJ, Bakker JA, de Koning M, Drukker M, Curfs LMG (2015): Glutamatergic markers, age, intellectual functioning and psychosis in 22q11 deletion syndrome. Psychopharmacol (Berl) 232:3319–3325.
63. Gothelf D, Feinstein C, Thompson T, Gu E, Penniman L, Van Stone E, *et al.* (2007): Risk factors for the emergence of psychotic disorders in adolescents with 22q11.2 deletion syndrome. Am J Psychiatry 164:663–669.
64. Weisman O, Guri Y, Gur RE, McDonald-McGinn DM, Calkins ME, Tang SX, *et al.* (2017): Subthreshold psychosis in 22q11.2 deletion syndrome: Multisite naturalistic study. Schizophr Bull 43:1079–1089.
65. Jalbrzikowski M, Murty VP, Tervo-Clemmens B, Foran W, Luna B (2019): Age-associated deviations of amygdala functional connectivity in youths with psychosis spectrum disorders: Relevance to psychotic symptoms. Am J Psychiatry 176:196–207.
66. Mesulam MM (1998): From sensation to cognition. Brain 121:1013–1052.
67. Córcoles-Parada M, Ubero-Martínez M, Morris RGM, Insausti R, Mishkin M, Muñoz-López M (2019): Frontal and insular input to the dorsolateral temporal pole in Primates: Implications for auditory memory. Front Neurosci 13:1099–1099.
68. Herath P, Kinomura S, Roland PE (2001): Visual recognition: Evidence for two distinctive mechanisms from a PET study. Hum Brain Mapp 12:110–119.
69. Schilbach L, Eickhoff SB, Rotarska-Jagiela A, Fink GR, Vogeley K (2008): Minds at rest? Social cognition as the default mode of cognizing and its putative relationship to the "default system" of the brain. Conscious Cogn 17:457–467.
70. van de Ven V (2013): Brain Functioning When the Voices Are Silent: Aberrant Default Modes in Auditory Verbal Hallucinations. In: Jardri R, Cachia A, Thomas P, Pins D, editors. The Neuroscience of Hallucinations. New York, NY: Springer, 393–415.
71. Beer JS (2007): The default self: Feeling good or being right? Trends Cogn Sci 11:187–189.
72. Esposito F, Aragri A, Latorre V, Popolizio T, Scarabino T, Cirillo S, *et al.* (2009): Does the default-mode functional connectivity of the brain correlate with working-memory performances? Arch Ital Biol 147:11–20.
73. Wible CG, Preus AP, Hashimoto R, Hashimoto R (2009): A cognitive neuroscience view of schizophrenic symptoms: Abnormal activation of a system for social perception and communication. Brain Imaging Behav 3:85–110.
74. Zhou L, Pu W, Wang J, Liu H, Wu G, Liu C, *et al.* (2016): Inefficient DMN suppression in schizophrenia patients with impaired cognitive function but not patients with preserved cognitive function. Sci Rep 6: 21657–21657.
75. Landin-Romero R, McKenna PJ, Salgado-Pineda P, Sarró S, Aguirre C, Sarri C, *et al.* (2015): Failure of deactivation in the default mode network: A trait marker for schizophrenia? Psychol Med 45:1315–1325.
76. Pomarol-Clotet E, Salvador R, Sarró S, Gomar J, Vila F, Martínez A, *et al.* (2008): Failure to deactivate in the prefrontal cortex in schizophrenia: Dysfunction of the default mode network? Psychol Med 38:1185–1193.

77. Binder JR (2012): Task-induced deactivation and the 'resting' state. NeuroImage 62:1086–1091.
78. Northoff G, Heinzel A, de Greck M, Bermpohl F, Dobrowolny H, Panksepp J (2006): Self-referential processing in our brain—A meta-analysis of imaging studies on the self. NeuroImage 31:440–457.
79. Whitfield-Gabrieli S, Moran JM, Nieto-Castañón A, Triantafyllou C, Saxe R, Gabrieli JDE (2011): Associations and dissociations between default and self-reference networks in the human brain. NeuroImage 55:225–232.
80. Deco G, Tononi G, Boly M, Kringelbach ML (2015): Rethinking segregation and integration: Contributions of whole-brain modelling. Nat Rev Neurosci 16:430–439.
81. He W, Sowman PF, Brock J, Etchell AC, Stam CJ, Hillebrand A (2019): Increased segregation of functional networks in developing brains. NeuroImage 200:607–620.
82. Baum GL, Ciric R, Roalf DR, Betzel RF, Moore TM, Shinohara RT, *et al.* (2017): Modular segregation of structural brain networks supports the development of executive function in youth. Curr Biol 27:1561–1572.e8.
83. Draganski B, Kherif F, Klöppel S, Cook PA, Alexander DC, Parker GJM, *et al.* (2008): Evidence for segregated and integrative connectivity patterns in the human basal ganglia. J Neurosci 28:7143–7152.
84. Yeo BTT, Krienen FM, Sepulcre J, Sabuncu MR, Lashkari D, Hollinshead M, *et al.* (2011): The organization of the human cerebral cortex estimated by intrinsic functional connectivity. J Neurophysiol 106:1125–1165.
85. Mancini V, Zöller D, Schneider M, Schaer M, Eliez S (2020): Abnormal development and dysconnectivity of distinct thalamic nuclei in patients with 22q11.2 deletion syndrome experiencing auditory hallucinations. Biol Psychiatry Cogn Neurosci Neuroimaging 5:875–890.
86. Delavari F, Sandini C, Kojovic N, Saccaro LF, Eliez S, Van De Ville D, *et al.* (2024): Thalamic contributions to psychosis susceptibility: Evidence from co-activation patterns accounting for intra-seed spatial variability (μCAPs). Hum Brain Mapp 45:e26649.
87. Koshino H, Minamoto T, Yaoi K, Osaka M, Osaka N (2014): Coactivation of the default mode network regions and Working Memory Network regions during task preparation. Sci Rep 4:5954–5954.
88. Li M, Dahmani L, Wang D, Ren J, Stocklein S, Lin Y, *et al.* (2021): Co-activation patterns across multiple tasks reveal robust anti-correlated functional networks. NeuroImage 227:117680–117680.
89. Damiani S, Fusar-Poli L, Brondino N, Provenzani U, Baldwin H, Fusar-Poli P, Politi P (2020): World/self ambivalence: A shared mechanism in different subsets of psychotic experiences? Linking symptoms with resting-state fMRI. Psychiatry Res Neuroimaging 299:111068.
90. Calamuneri A, Arrigo A, Mormina E, Milardi D, Cacciola A, Chillemi G, *et al.* (2018): White matter tissue quantification at low b-values within constrained spherical deconvolution framework. Front Neurol 9: 716–716.
91. Smith RE, Tournier J-D, Calamante F, Connelly A (2012): Anatomically-constrained tractography: Improved diffusion MRI streamlines tractography through effective use of anatomical information. NeuroImage 62:1924–1938.
92. Smith RE, Tournier JD, Calamante F, Connelly A (2015): The effects of SIFT on the reproducibility and biological accuracy of the structural connectome. NeuroImage 104:253–265.
93. Yeh CH, Smith RE, Liang X, Calamante F, Connelly A (2016): Correction for diffusion MRI fibre tracking biases: The consequences for structural connectomic metrics. NeuroImage 142:150–162.
94. Wechsler D, Kodama H (1949). Wechsler Intelligence Scale for Children, 1. New York: Psychological Corporation.
95. Wechsler D (1955): Wechsler Adult Intelligence Scale. New York: Psychological Corporation.
96. Reich W (2000): Diagnostic interview for children and adolescents (DICA). J Am Acad Child Adolesc Psychiatry 39:59–66.
97. Kaufman J, Birmaher B, Brent D, Rao U, Flynn C, Moreci P, *et al.* (1997): Schedule for affective disorders and schizophrenia for school-age children-present and lifetime version (K-SADS-PL): Initial reliability and validity data. J Am Acad Child Adolesc Psychiatry 36:980–988.
98. First MB, Spitzer RL, Gibon F-M, Williams J (2002): Structured Clinical Interview for DSM-IV-TR Axis I Disorders, Research Version (SCID-I RV). New York: New York State Psychiatric Institute.